Experimental Parasitology 265 (2024) 108811

Contents lists available at ScienceDirect

Experimental Parasitology

journal homepage: www.elsevier.com/locate/yexpr

PLGA-PEG-COOH nanoparticles are efficient systems for delivery of mefloquine to *Echinococcus multilocularis* metacestodes

Brice Autier [a], Alexis Verger [b,1], Charleen Plaisse [c], Christelle Manuel [c], Marylène Chollet-Krugler [b], Matias Preza [d], Britta Lundstroem-Stadelmann [d,e], Marian Amela-Cortes [b], Caroline Aninat [f], Michel Samson [c], Nolwenn Brandhonneur [b], Sarah Dion [c,*]

[a] IRSET (UMR_S 1085), INSERM (Institut de Recherche en Santé, Environnement et Travail), EHESP, CHU Rennes, University of Rennes, Rennes, France
[b] CNRS, ISCR (Institut des Sciences Chimiques de Rennes)-UMR 6226, Univ Rennes, F-35000, Rennes, France
[c] IRSET (UMR_S 1085), INSERM (Institut de Recherche en Santé, Environnement et Travail), EHESP, University of Rennes, Rennes, France
[d] Institute of Parasitology, Department of Infectious Diseases and Pathobiology, Vetsuisse Faculty, University of Bern, Bern, Switzerland
[e] Multidisciplinary Center of Infectious Diseases, University of Bern, Berne, Switzerland
[f] INSERM, Université Rennes, INRAE, Institut NuMeCan, Nutrition, Metabolisms and Cancer, F-35000, Rennes, France

ARTICLE INFO

Keywords:
poly(lactic co-glycolic acid)
Drug delivery system
Alveolar echinococcosis
EmPGI
Drug therapy

ABSTRACT

Alveolar echinococcosis (AE) is a severe disease caused by the infection with the larval stage of *Echinococcus multilocularis*, the metacestode. As there is no actual curative drug therapy, recommendations to manage AE patients are based on radical surgery and prophylactic administration of albendazole or mebendazole during 2 years to prevent relapses. There is an urgent need for new therapeutic strategies for the management of AE, as the drugs in use are only parasitostatic, and can induce toxicity. This study aimed at developing a drug delivery system for mefloquine, an antiparasitic compound which is highly active against *E. multilocularis in vitro* and in experimentally infected mice. We formulated mefloquine-loaded PLGA-PEG-COOH (poly-(lactic-co-glycolic acid)) nanoparticles that exhibit stable physical properties and mefloquine content. These nanoparticles crossed the outer acellular laminated layer of metacestodes *in vitro* and delivered their content to the inner germinal layer within less than 5 min. The *in vitro* anti-echinococcal activity of mefloquine was not altered during the formulation process. However, toxicity against hepatocytes was not reduced when compared to free mefloquine. Altogether, this study shows that mefloquine-loaded PLGA-PEG-COOH nanoparticles are promising candidates for drug delivery during AE treatment. However, strategies for direct parasite-specific targeting of these particles should be developed.

1. Introduction

Alveolar echinococcosis (AE) is one of the most lethal helminthiases worldwide (Casulli, 2020). The infection with the larval stage of *Echinococcus multilocularis*, the metacestode, is caused upon ingestion of parasite eggs, which are released into the environment with feces of final hosts (wild canids, mainly foxes). The metacestodes grow mainly in the liver of intermediate hosts such as rodents, but also aberrant hosts including humans. They form of a heterogeneous mass composed of parasite microcysts intermingled with host connective tissue. These fluid filled microcysts are composed of two layers: the inner the germinal layer (GL), which contains viable parasite tissue including connective tissue cells, muscle cells, glycogen storage cells, neuronal cells and undifferentiated stem cells, and the outer acellular laminated layer (LL), which is composed of tight meshwork of high molecular mass mucopolysaccharides (Lundström-Stadelmann et al., 2019). In humans, the host immune response that develops at the periphery of the parasite is a granulomatous response with a strong infiltration of immune cells (macrophages, lymphocytes) and stromal cells (fibroblasts, endothelial cells) (Vuitton et al., 2006). In most cases, the early Th1-dominated immune response is able to clear the infection, but in some individuals the metacestode is able to induce an immune switch towards a

* Corresponding author.
E-mail address: sarah.dion@univ-rennes.fr (S. Dion).
[1] Actual affiliation: UPR CNRS 4301 CBM, département NMNS, Université de Tours, 37200 Tours, France.

https://doi.org/10.1016/j.exppara.2024.108811
Received 5 April 2024; Received in revised form 10 June 2024; Accepted 5 August 2024
Available online 5 August 2024

Th2-dominated and non-inflammatory host response, which allows the parasite to grow indefinitely. In most cases, AE is fatal if not treated appropriately (Gottstein et al., 2015; Vuitton et al., 2020). Due to the slow growth of the parasite, AE is often diagnosed years or decades post-infection, and at this stage metacestodes are often characterized by peripheral fibrosis and central necrosis and calcifications (Vuitton et al., 2006).

The recommended management of AE consists of radical surgery combined with prophylactic chemotherapy by the benzimidazoles albendazole or mebendazole during at least 2 years post-surgery (Brunetti et al., 2010). These drugs have been used for AE treatment since more than 40 years (Schantz et al., 1982). While benzimidazoles have clearly had an impact and increased the life expectancy of quality of life of AE patients, they have significant drawbacks. They act parasitostatic only, meaning that in the vast majority of patients an interruption of the treatment leads to the metacestode recurrence (Lundström-Stadelmann et al., 2019). Additionally, although these drugs are generally well-tolerated, they are poorly absorbed, and blood levels in different patients can be variable, thus constant monitoring and adjustement of the treatment dose is warranted. Moreover, due to the chronicity of treatment, benzimidazoles are prone to induce liver injury and other adverse side-effects (e.g. alopecia, bone marrow aplasia), which can lead to treatment discontinuation (Burkert et al., 2022). For these reasons, there is an urgent need for new drugs and therapeutic strategies for the treatment of AE.

Many compounds were previously evaluated for their activity against *E. multilocularis* metacestodes. These included, anti-infective agents such as di-cationic pentamidine derivatives, buparvaquone, artemisinin derivatives and mefloquine (Küster et al., 2013; Rufener et al., 2018a; Spicher et al., 2008; Stadelmann et al., 2016), anti-cancer drugs e.g. imatinib, nilotinib, everolimus and bortezomib (Hemer and Brehm, 2012; Joekel et al., 2018; Stadelmann et al., 2014) and other agents (Gao et al., 2021; Liu et al., 2021; Loos et al., 2020). Among them, mefloquine has emerged as a promising candidate as it exhibits parasiticidal activity *in vitro* (Küster et al., 2011, 2015; Lundström--Stadelmann et al., 2020; Memedovski et al., 2023; Rufener et al., 2018b; Stadelmann et al., 2011). In mice that were experimentally infected through intraperitoneal injection of metacestode tissue or oral application of *E. multilocularis* eggs, mefloquine was as effective as the standard albendazole treatment (Küster et al., 2015; Rufener et al., 2018b). These results suggested that mefloquine could be a promising alternative to benzimidazoles.

However, the pharmacokinetics of the drug needs to be improved. Indeed, beyond digestive absorption, the hepatic metabolism and the binding to serum proteins, the drug has to pass through the fibrosis, the necrosis and the outer laminated layer of the parasite, composed of mucopolysaccharides, to access the germinal layer which represents the live metacestode tissue (Vuitton et al., 2020). With this aim, we developed mefloquine-loaded polymeric nanoparticles of PLGA (poly-(-lactic-co-glycolic acid)), which is a well characterized and FDA-approved pharmaceutical formulation (Verger et al., 2022; Wang et al., 2021). The choice of PLGA relied on the hydrophobicity of mefloquine (logP: 4.11), which was compatible with a loading into the hydrophobic core of this type of nanoparticles. Additionally, the biocompatibility and biodegradability of PLGA make it a good candidate for nanomedicine. PLGA has excellent biodistribution properties and accumulates in the liver (Li et al., 2023; Semete et al., 2010). Moreover, it was shown recently that application of PLGA nanoparticles containing the incorporated carbazole aminoalcohol compound H1402 reduced parasite growth in a mouse model of liver infection (Li et al., 2023). Thus, PLGA nanoparticles could be exploited as nanocarriers that are able to reach the parasite in the liver, and are thus of interest for AE treatment. Altogether, these data show that mefloquine is a promising treatment but its pharmacokinetics should be modified for AE treatment, and that PLGA nanoparticles could be a solution for this.

We here report on the preparation of a mefloquine-PLGA formulation, show that PLGA nanoparticles are readily taken up by *E. multilocularis* metacestodes, and study the *in vitro* activity of mefloquine-PLGA employing *in vitro* cultured *E. multilocularis* metacestodes as well as *in vitro* cytotoxicity in human liver cells. This work serves as a basis for further *in vivo* applications. Altogether, we showed that nanoparticle-based drug delivery is a promising therapeutic strategy, which could be performed with mefloquine, its derivatives or other drugs with anti-echinococcal activity (Lundström-Stadelmann et al., 2019).

2. Materials and methods

2.1. Chemicals

Acid terminated PLGA 50:50 MW 24,000–38,000 (Resomer® RG503H), anhydrous dichloromethane, dicyclohexylcarbodiimide (DCC), N-hydroxysuccinimide (NHS), diethyl ether, poly(ethylene glycol 2000) (PEG, 2000) bis(amine), dimethylaminopyridine, succinic anhydride, triethylamine, hydrochloric acid, magnesium sulphate, polysorbate, coumarine-6 and dimethylsulfoxide (DMSO) were purchased from Sigma Aldrich (Saint-Quentin-Fallavier, France). Mefloquine hydrochloride was purchased from Selleck Chemicals (Houston, TX, USA). Analytical reagent grade methanol, acetone, acetonitrile and formic acid were obtained from VWR international S.A.S. (Fontenay-sous-Bois, France).

2.2. Synthesis and characterization of PLGA-PEG-COOH polymer

2.2.1. Activation of COOH group on PLGA

Dissolved PLGA in anhydrous dichloromethane was reacted with DCC and NHS for 24 h at room temperature (RT) under argon atmosphere at a stochiometric molar ratio of PLGA:DCC:NHS of 1:10:10. The by-product N,N′-dicyclohexylurea was removed by filtering through a 0.45-μm Teflon® syringe filter. The filtrate was precipitated and washed with ice-cold diethyl ether. The precipitate was vacuum-dried to obtain activated PLGA.

2.2.2. Conjugation of PEG with activated PLGA

Activated PLGA and PEG 2000 bis(amine) were dissolved in anhydrous dichloromethane (1:1 mol-mol ratio) and reacted overnight at RT under argon. The reaction mixture was precipitated and washed with cold methanol. The precipitate was then vacuum dried to obtain PLGA-PEG-NH_2.

2.2.3. Functionalization with COOH radical

Based on the work of Amela-Cortes et al. (2011), PLGA-PEG-NH_2 (300 mg), dimethylaminopyridine (65 mg) and succinic anhydride (43 mg) were mixed and dried under vacuum for 1 h. Afterwards, triethylamine (43 mg) was added and the mixture was dissolved in anhydrous dichloromethane. The reaction was stirred overnight under argon. The crude was then successively washed 3 times with hydrochloric acid at pH = 3, 3 times with water and finally 3 times with brine. The organic layer was dried over magnesium sulphate, the solvent evaporated and PLGA-PEG-COOH was isolated with a 99.7% yield.

2.2.4. Characterization of PLGA-PEG-COOH polymer

PLGA, PLGA-PEG-NH_2 and PLGA-PEG-COOH copolymers were analyzed by Fourier-Transform-Infrared (FT-IR) using the VERTEX 70v FT-IR spectrometer (Bruker, Wissembourg, France) with the following parameters: scan range 4400–400 cm^{-1}, number of scans 16, resolution 4.0 cm^{-1}, interval 1.0 cm^{-1} and unit %T. Copolymers were also analyzed by proton nuclear magnetic resonance (^{1}H NMR) spectroscopy using the Bruker Avance 400 MHz NMR spectrometer (Bruker, Wissembourg, France). The thermal behavior of synthesized copolymer was studied by differential scanning calorimetry (DSC) on a Discovery DSC-25 device (TA instruments, New Castle, USA). Samples (approximately

5 mg) were weighed and placed in aluminum pans before sealing. Using nitrogen as protective gas, samples were heated at a constant rate of 10 °C/min in a temperature range of 0 °C–200 °C. The thermogram curves were analyzed with the TRIOS software v5.0 (TA instruments, New Castle, USA).

2.3. Nanoparticles formulation and characterization

2.3.1. Nanoparticles formulation

An organic solution in acetone (4 g) of PLGA-PEG-COOH polymer (25 mg), polysorbate 20 (75 mg) and either coumarine-6 (13 mg) or mefloquine hydrochloride (13 mg), was slowly added to 15 mL of Water for Injection (0169 according to European Pharmacopoeia) with a 5 mL syringe and a 25G needle (Terumo Europe, Leuven, Belgium) under magnetic stirring (450 rpm) at room temperature (20–25 °C). In these conditions, a bluish colloidal nanosuspension formed instantaneously due to the ouzo effect (Ganachaud and Katz, 2005). The acetone was then removed under reduced pressure (200 mBar) by a rotary evaporator Laborata 4000 (Heidolph, Schwabach, Germany) for 1 h. The nanosuspensions were purified by centrifugation (5000 *g*, 10 min) to eliminate polymer aggregates and precipitated reagents. They were stored at 4 °C for stability study, and an aliquote was stored at −80 °C at each timepoint for further drug dosage. Before each stability and *in vitro* experiment, the formulation was dialyzed against 500 mL of deionized water using a pre-wetted Spectra/Por™ Float-a-Lyzer™ G2 device with a molecular weight cutoff of 20 kDa (Spectrum™, Repligen™, Castanet Tolosan, France), in order to eliminate free and released compounds.

2.3.2. Nanoparticles characterization

Sizes and zeta potentials of nanoparticles were checked for each batch of nanoparticles using the Malvern Zetasizer Nano ZS device (Malvern Instruments, Malvern, United Kingdom). A calibration curve for dosage of mefloquine in nanoparticles solutions was established by dilutions of a 4 g/L (9.64 mM) initial solution with acetonitrile in order to have 120 mg/L, 160 mg/L, 200 mg/L, 240 mg/L and 280 mg/L standard solutions. Samples were diluted at 1:10 with acetonitrile before analysis, which solubilized nanoparticules. Mefloquine concentrations were determined using the 1220 Infinity II LC system (Agilent Technologies™, Dako, Les Ulis, France) with the InfinityLab Poroshell SB-C18 column (150 × 4.6 mm, i.d. 4 µm, Agilent Technologies™) and the Diode Array Detector for UV detection at 220 nm. The mobile phase consisted of 50% of A (0.1% formic acid in water) and 50% of B (0.1% formic acid in acetonitrile). Flow rate was 1 mL/min and 10 µL of each sample was injected. Analysis was done using the Lab Advisor software (Agilent Technologies™, Dako, Les Ulis, France). Mefloquine was quantified by measuring Area Under the Curve (AUC) at 220 nm at the retention time of the standard mefloquine (Rt = 2.4 min) and by using the calibration curve.

2.4. Parasite material

2.4.1. Ethics statement

All experimental protocols on animals were conducted in compliance with the French laws (Décret n° 2013-118), the institution's guidelines for animal welfare, and European recommendations from the EEC Council Directive 2010/63/EU. Authors were given permission to conduct animal experimentation by "La direction des Services Vétérinaires", the project was reviewed and authorized by the "Comité d'Ethique en Expérimentation Animale" (C2EA-07), and license was given by the "Ministère de l'Enseignement Supérieur, de la Recherche et de l'Innovation", #28586–202011261535409.

2.4.2. Animals and infection procedure

Animals were housed in individual cages in specific pathogen-free conditions in a conventional animal facility (Arche platform, Biosit, Rennes) with a 12 h dark-light cycle, at 25 °C, 50% relative humidity and HEPA-filtered air (Forma Scientific, Marietta, OH), with food (2016 Teklad global 16% protein rodent diets, Envigo, Gannat, France) and water *ad libitum*. The *E. multilocularis* isolate H95 was maintained *in vivo* by serial peritoneal infections of BALB/c mice (Janvier Laboratories, Le Genest-Saint-Isle, France) also at the Rennes animal facility. Metacestodes were collected from an infected mouse, crushed and sieved to remove debris. After an overnight sedimentation in PBS containing 100 U/mL penicillin and 100 U/mL streptomycin (Gibco™, Thermo Fisher Scientific, Illkirch, France) at 4 °C, the pellet was washed with PBS and centrifuged 5 min 500 *g* at 4 °C. The metacestodes in the final pellet weresuspended in culture medium (same as described in "Primary metacestode culture" subsection). They were then applied for either intraperitoneal inoculation of 5 uninfected mice, or were used for *in vitro* primary culture (Stadelmann et al., 2010a).

2.4.3. Primary metacestode culture

For primary metacestode culture, metacestodes obtained from an infected mouse were suspended in 20 mL of DMEM high glucose, pyruvate (Gibco™, Thermo Fisher Scientific, Illkirch, France), supplemented in 10% fetal calf serum (FCS, Eurobio Scientific, Les Ulis, France), 10 mg/L tetracycline (Sigma Aldrich, Saint-Quentin-Fallavier, France), 100 U/mL penicillin and 100 U/mL streptomycin (Gibco™, Thermo Fisher Scientific, Illkirch, France), and co-cultured with Reuber rat hepatoma (Rh) cells (ATCC #H4-II-E-C3) in culture flasks at 37 °C under 5% CO_2, as previously described (Stadelmann et al., 2010b). One to two month-old metacestode vesicles were isolated and washed with PBS prior to further experiments.

2.4.4. Assessment of nanoparticle entry by fluorescence testing

In order to assess if nanoparticles pass through the laminated layer of the parasite, we exposed *E. multilocularis* metacestodes *in vitro* to coumarine-6-loaded PLGA-PEG-COOH nanoparticles and detected fluorescence from both the vesicle fluid and germinal layer cells. The vesicle fluid was collected by mechanical lysis and centrifugation, and cell extract was obtained by trypsinization and chemical lysis of the vesicule membranes. In a 2 mL tube, 500 µL of *in vitro* cultured *E. multilocularis* vesicles were exposed to 500 µL of a 1:1 dilution in PBS of either coumarine-6-loaded or unloaded PLGA-PEG-COOH nanoparticles for 30 min, 90 min or 24 h at RT in the dark. The supernatant was sampled, the vesicles were washed 3 times with PBS and the third washing supernatant was sampled. The remaining PBS was removed by careful pipetting, the vesicles were broken, the whole suspension was centrifuged at 500 *g* for 5 min (RT) and the supernatant (vesicle fluid) was sampled. The pellet containing laminated and germinal layer was suspended in 200 µL of trypsin-EDTA 0.25% (Gibco™, Thermo Fisher Scientific, Illkirch, France) and incubated 5 min at RT with gentle manual shaking. The suspension was then filtered through 70 µm cell strainers (Corning™, Sigma-Aldrich, Saint-Quentin-Fallavier, France), the filtrate was centrifuged at 500 *g* for 5 min (RT), washed with PBS, and after another centrifugation at 500 *g* for 5 min, the pellet was lysed by 90 µL of a 1% solution of Triton X-100™ in PBS (cell extract). Finally, optical density of 90 µL of each sample (nanoparticles solution, third wash, vesicular fluid, cell extract) was measured at 520 nm under excitation at 450 nm in a black 96-well plate. Three independent experiments were conducted at the University of Rennes.

2.4.5. Assessment of nanoparticles entry by confocal microscopy

In vitro cultured *E. multilocularis* vesicles were distributed in 12 well culture plates and exposed to a 1:1 dilution in PBS of either coumarine-6-loaded or unloaded PLGA-PEG-COOH nanoparticles for 5 min, 15 min and 30 min at RT in the dark. Samples were washed in PBS, fixed in formalin 4% and re-suspended in PBS. Exposed vesicles were immediately processed in ibidi™ µ-Slide Angiogenesis with glass bottom (ibidi™, Munich, Germany) and analyzed using a Leica™ TCS SP8 confocal microscope (Leica™, Mannheim, Germany). Wavelengths of excitation and emission were 488 nm (argon laser) and 500 nm,

respectively. Two independent experiments were conducted at the University of Rennes.

2.5. Assessment of mefloquine and mefloquine-PLGA-PEG-COOH formulations against E. multilocularis metacestodes in vitro

2.5.1. In vitro drug treatment

To quantitatively assess the damage induced by free mefloquine and mefloquine loaded in nanoparticules (mefloquine and mefloquine-NP, respectively), the previously described PGI assay was employed (Stadelmann et al., 2010a). Intact 2–4 mm vesicles were isolated by flotation using 2% saccharose solution, extensively washed with PBS and diluted 1:1 with DMEM without phenol red (Seraglob, Bioswisstec, Schaffhausen, Switzerland). One milliter of metacestode vesicles per well were cultured in 48-well culture plate at 37 °C under 5% CO_2 and exposed to 30 μM (EC_{50} as reported by (Stadelmann et al., 2016)) or 60 μM of either mefloquine or mefloquine-NP. Negative controls were exposed to 2% DMSO or to 0.4% blank nanoparticles (without drug), corresponding to the highest concentrations of vehicles for free and loaded mefloquine, respectively. Positive controls were vesicles exposed to 1% Triton X-100. Five and 14 days later, 120 μL of supernatant was sampled, and finally vesicles were crushed and 120 μL of supernatant was sampled again. All the supernatants were stored frozen at −20 °C until further analysis. Two independent experiments were conducted, one at the University of Rennes, the other at the University of Bern, each with three biological replicas.

2.5.2. Enzymatic assay

The impact of mefloquine and mefloquine-NP was evaluated *in vitro* by indirect detection of the released EmPGI-activity by damaged metacestodes, as previously described (Stadelmann et al., 2010a). The EmPGI assay is one of the most reliable technique for assessment of drug activity against *E. multilocularis* metacestodes. Indeed, it relies on the kinetics of the enzymatic reaction, whereas other assays (e.g. EmALP assay) rely on the endpoint detection of the product (Stettler et al., 2001), which is not directly proportional to the enzymle concentration.

The EmPGI assay is based on an enzymatic reaction initiated by the addition of fructose-6-phosphate to a mix containing EmPGI (putatively in supernatant), $4{,}4.10^{-1}$ mM β-nicotinamide adenine dinucleotide hydrate, 1,8 U/mL glucose-6-phosphate dehydrogenase, $8{,}8.10^{-1}$ mM EDTA and 100 mM Tris-HCl (all reagents from Sigma Aldrich, Saint-Quentin-Fallavier, France). In the presence of EmPGI, $NADH,H^+$ was generated and detected continuously during 30 min at an absorbance of 340 nm using a SPECTROstar™ Nano spectrophotometer (BMG Labtech, Champigny sur Marne, France). A nonlinear regression curve was fitted using GraphPad Prism software v8.0.2 (GraphPad, La Jolla, CA, USA). Drug activity was calculated as proportion of released EmPGI expressed as % Triton X-100 using Microsoft Office Excel 2019 (Microsoft France, Issy-les-Moulineaux, France).

2.6. Cytotoxicity of mefloquine and mefloquine-PLGA-PEG-COOH formulations against human hepatoma cells in vitro

Differentiated HepaRG cells were obtained as previously described (Gripon et al., 2002), and cultured in an opaque 96-well flat-bottom plate, in William's medium E (Eurobio Scientific, Les Ulis, France), supplemented in 10% FCS (Perbio Science, Villebon-Sur-Yvette, France), 100 U/mL penicillin and 100 U/mL streptomycin (Gibco™, Thermo Fisher Scientific, Illkirch, France), 5 μg/mL insulin (Sigma Aldrich, Saint-Quentin-Fallavier, France) and 2% DMSO (Gripon et al., 2002). Each well was seeded with 2-3 x 10^5 cells and cultures were maintained at 37 °C under 5% CO_2. Cells were exposed to mefloquine or mefloquine-NP, in a range of concentrations from 1 μM to 70 μM, without DMSO (or less than 0.7% for mefloquine), during 48h. The positive control was cells exposed to 1% Triton X-100 and negative controls were cells exposed to either William's Medium E with DMSO, with blank PLGA-PEG-COOH nanoparticles, or without any additional compound. Cell viability was evaluated by quantification of ATP, using the CellTiter-Glo® assay (Promega, Charbonnières-les-Bains, France). This assay was used following manufacturer's recommendation and luminescence was quantified using a multimode microplate reader ClarioSTAR (BMG Labtech, Champigny-sur-Marne, France). Data were expressed as % of the luminescence of the negative control. One experiment with three biological replica was conducted at the University of Rennes.

2.7. Statistical analysis

Statistical analysis and plots of data were done using GraphPad Prism software v8.0.2 (GraphPad, La Jolla, CA, USA). The α risk was set to 0.05 for all analyses, and the same representation of significance was used throughout the manuscript: *$p < 0.05$, **$p < 0.01$ and ***$p < 0.001$. Stability of each physical characteristic of the mefloquine-NP was analyzed using the non-parametric Friedman test for paired data, with *post-hoc* Dunn's multiple comparisons test. Fluorescence intensities and antiparasitic activities were compared using the two-way ANOVA test and the one-way ANOVA test, respectively. *Post-hoc* analysis compared all compounds to each other within a timepoint using the Tukey's or Bonferonni's multiple comparison test, as specified. Dose-response curve for toxicity evaluation and LC_{50} (concentration with 50% dead cells) were determined by extrapolation of a non-linear four-parameter dose-response curve.

3. Results

3.1. Characterization of PLGA-PEG-COOH polymer

The successful formation of PLGA-PEG-COOH polymer was confirmed by FT-IR (Fig. 1A). The overall spectral pattern was unchanged post grafting of PLGA-PEG-NH_2. After addition of a -COOH terminal group, the spectra exhibited a broad O-H stretching at 3200–3650 cm^{-1}, C=O stretching at 1720 cm^{-1} and C-O stretching at 1050 cm^{-1} which corresponded to carboxylic groups.

Differential scanning calorimetry (DSC) measurements were performed on copolymers, to investigate differences of the glass transition temperature (T_g) during chemical transformation (Fig. 1B). For native PLGA, T_g was around 36.1 °C and decreased to 30.4 °C after grafting of PLGA-PEG-NH_2. This decrease is in accordance with the addition of flexible ethyleneglycol units. After transformation to PLGA-PEG-COOH copolymer, the Tg increased again to 34.9 °C. These slight variations showed that the chemical transformation was effective, without radical modification of this physical characteristic.

The successful formation of PLGA-PEG-COOH copolymer was confirmed by characterizing this copolymer by ^1H NMR (Fig. 1C). Comparison of the spectra of PLGA-PEG-NH_2 with PLGA showed signals corresponding to the carbons of the ethylenic groups of the PEG backbone at 3.6 ppm. The spectrum of PLGA-PEG-COOH showed the appearance of a supplementary band at 2.19 ppm that correspond to the CH_2CH_2COOH terminal groups of the copolymer.

3.2. Characterization of nanoparticles

At synthesis, the size of the mefloquine-NP was 96.6 ± 9.0 nm with a low polydispersity index (PDI) of 0.13 ± 0.02 (monodisperse system if PDI <0.2 (Caputo et al., 2019)) and a satisfying (<30 mV) zeta potential of 12.7 ± 3.4 mV (Fig. 2A). Size and PDI were stable during at least 45 days. After a slight decrease during the first week (not significant using ANOVA test), loading of mefloquine was stable during at least 3 months at 4 °C (Fig. 2B) and was 68.9 ± 3.9 %, which was equivalent to a suspension with a mean concentration of 2.2 ± 0.1 mM of mefloquine.

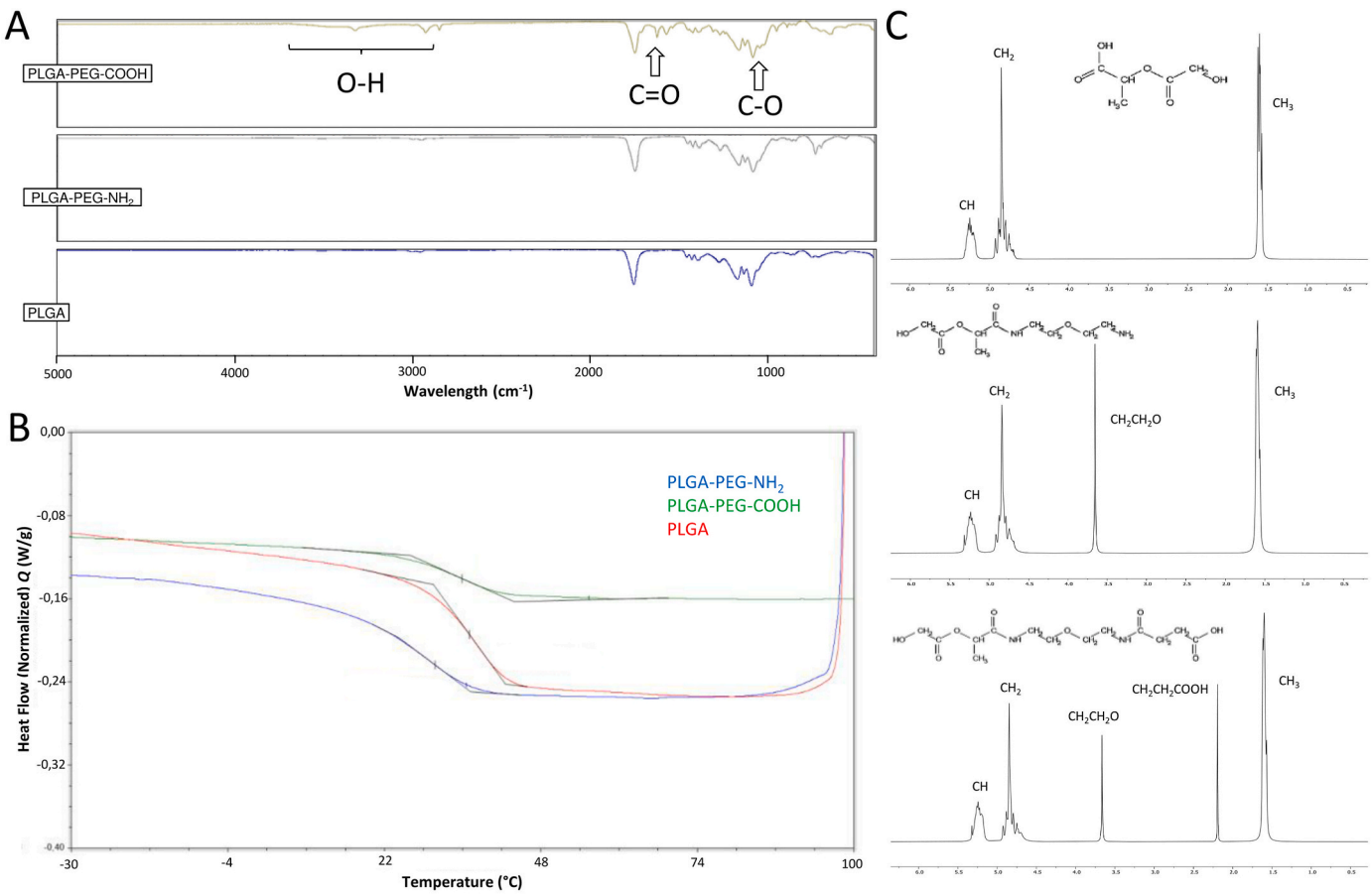

Fig. 1. Chemical validation of PLGA-PEG-COOH polymer. (A) Fourier Transform-Infrared spectra of PLGA-PEG-COOH, PLGA-PEG-NH_2 and PLGA. The typical stretchings for O-H, C=O and C-O bounds were annotated. (B) Differential scanning calorimetry thermograms of PLGA polymers. (C) ^{1}H NMR spectra of PLGA (top), PLGA-PEG-NH_2 (middle) and PLGA-PEG-COOH (low) copolymer in $CDCl_3$. Each peak is annotated with the corresponding group.

3.3. Entry of PLGA nanoparticles into E. multilocularis metacestodes

After exposition of *E. multilocularis* metacestodes to coumarine-6-loaded nanoparticles during 30 min (Fig. 3A), fluorescence was detected in the germinal layer cell extract, and, to a lesser extent, in vesicle fluid (Fig. 3B). After 90 min of exposition, similar fluorescence levels were detected vesicle fluid germinal layer cell extract (Fig. 3B), and after 24 h, fluorescence levels had increased in cell extract and vesicle fluid (Fig. 3B). No fluorescence was detected in vesicles not exposed to coumarine-6-loaded nanoparticles.

Confocal microscopy showed that 5 min of exposition was sufficient to detect coumarine-6 in germinal layer cells (Fig. 3C). Fluorescence was not observed in the laminated layer at any of the timepoints investigated (30 min (Figs. 3C), 90 min (data not shown)). No fluorescence could be seen in metacestodes exposed to blank PLGA-PEG-COOH nanoparticles.

3.4. In vitro activity against E. multilocularis metacestodes

After 5 days of exposition to 30 μM or 60 μM mefloquine, EmPGI release from the metacestodes was 90.2 ± 17.8 % and 108.9 ± 10.6 % of the internal Triton X-100 control, respectively (Fig. 4A). The same exposition time to 30 μM and 60 μM mefloquine-NP lead to 39.7 ± 26.5 % ($p < 0.05$ vs 30 μM mefloquine, $p < 0.01$ vs 60 μM mefloquine) and 103.4 ± 13.9 % ($p < 0.01$ vs 30 μM mefloquine-NP) of EmPGI, respectively. Except for 30 μM mefloquine-NP, all conditions had exerted significant anti-parasitic activity when compared to the negative controls ($p < 0.001$). Similar results were obtained after a treatment lasting 12 days (Fig. 4A). Microscopical observation of the metacestodes showed that *E. multilocularis* vesicles exposed to both mefloquine and mefloquine-NP at 60 μM were damaged, in contrast to vesicles exposed to DMSO or blank nanoparticles (Fig. 4B).

3.5. Cytotoxicity in human hepatoma HepaRG cells

Toxicity of free mefloquine or mefloquine-NP was evaluated by quantifying viability of exposed human hepatoma HepaRG cells (Fig. 4C). Formulation of mefloquine into nanoparticles did not alter toxicity as the LC_{50} after 48h exposition was 31.7 ± 4.2 μM for free mefloquine, and 30.8 ± 7.4 μM for mefloquine-NP. DMSO and blank nanoparticles did not have significant impact on cell viability (data not shown).

4. Discussion

Treatment of AE is suffering from a lack of therapeutic possibilities, especially in terms of available and efficient antiparasitic drugs. In this proof of principle study, we aimed at developing a nanovectorized formulation of mefloquine, previously shown to have promising *in vitro* and *in vivo* activity (Küster et al., 2015; Lundström-Stadelmann et al., 2020; Rufener et al., 2018b). We focused (i) on a non-benzimidazole drug, which could be administered to patients suffering from benzimidazole-related side effects, and (ii) on an already used drug in human medicine, to increase its chance to be introduced in the market. Mmefloquine was reproducibly formulated in PLGA-PEG-COOH nanoparticles, and the physical properties of the formulation as well as the loading of nanoparticles with mefloquine remained stable for atleast 45 days. Size, PDI and zeta potential were compatible with an *in vivo* administration. In addition, PLGA-PEG-COOH nanoparticles were able

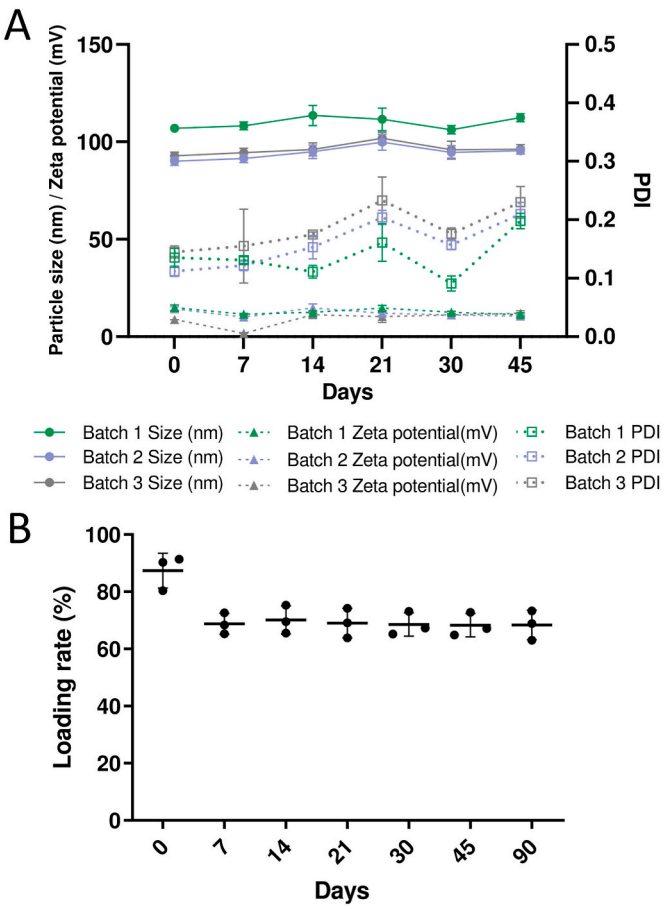

Fig. 2. Stability of the mefloquine-loaded PLGA nanoparticles. (A) Physical characteristics of the mefloquine-loaded PLGA nanoparticles. Once formulated, nanoparticles were stored at 4 °C in the dark and reanalyzed at each time point. Data are expressed as m ± SD of 3 independent experiments. PDI polydispersity index. (B) Mefloquine loading stability of PLGA-PEG-COOH nanoparticles. Cumulative data of 3 independent experiments. Plot shows mean and SD.

to cross the laminated layer and reached the germinal layer of the parasite *in vitro* in less than 5 min. At 60 μM mefloquine concentration, treatments with free mefloquine and the mefloquine NP formulation induced similar levels of EmPGI activity. However, at 30 μM, EmPGI release for the mefloquine-NP formulation was at a lower level compared to free mefloquine, indicating the NP-associated drug induced less physical damage. This was expected *in vitro*, since the PLGA-nanoparticles have to undergo degradation in order to release their content, while free mefloquine enters the parasite by simple diffusion. *In vivo*, this effect could be compensated by enhancing the biodistribution of the particles through targeting them closer to the infections site, thus applying targeted treatment rather than systemic approaches.

The same would account for preventing adverse side effects, due to unspecific cytotoxicity. We showed that loading mefloquine into PLGA-PEG-COOH nanoparticles did not have any impact on the toxicity in a HepaRG cell line. Both free and NP-bound mefloquine altered the viability of these cells at a similar LC_{50} range as the EC_{50} in metacestodes determined by PGI assay. However, cytotoxicity values can differ between different cell types and cell lines of different tissue origin, and further investigations are needed to obtain a clearer picture. The dosage of mefloquine that can be applied in humans and in animal models is limited, due to its potential toxicity (Ghosh et al., 2021). Of note, the main toxic effects described for mefloquine are neurological and psychiatric disorders, but the underlying mechanisms are not fully understood yet (Martins et al., 2021).

For a future application of these nanoparticles, a targeting strategy needs to be applied, in order to increase the delivery of these particles close to the parasite and to decrease the distribution to susceptible tissues. With this in mind, we evaluated activities of PLGA-PEG-COOH nanoparticles instead of the older-generation PLGA nanoparticles (Venier-Julienne and Benoît, 1996). PLGA nanoparticles are known to be easily opsonized and cleared by the reticular endothelial system, and PEGylation of the nanoparticles, as done in our study, increases their biological half-life (Zhang et al., 2022). Engraftment of a -COOH radical was not guided by a pharmacokinetic need, but this group could be utilized for conjugation of an antigen-binding protein, e.g. a monoclonal antibody (mAb) (Lee et al., 2022), that would allow parasite-specific targeting of these nanoparticles (Friedman et al., 2013). This strategy could allow to specifically target the stem cells of *E. multilocularis*, which are the key players for metacestode survival, dissemination and also relapse (Koziol and Brehm, 2015).

Additional studies in AE mouse models for hepatic infection will have to address the biodistribution of mefloquine-NPs, especially in relation to the periparasitic fibrosis that could potentially hinder access to the metacestodes *in vivo* (N. Yang et al., 2022). It is highly suspected that periparasitic fibrosis could limit drug delivery, since immunocompromised patients, who develop a weaker periparasitic response (including fibrosis), are more responsive to benzimidazole treatments (Autier et al., 2023; Chauchet et al., 2014).

Few studies have evaluated drug delivery systems for treatment of AE. The first one evaluated doxorubicin-loaded poly-isohexylcyanoacrylate nanoparticles (Liance et al., 1993), followed by multiple formulations of albendazole, showing that albendazole-loaded nanoparticles exhibited increased efficacy, allowing lower dosage of the drug (Abulaihaiti et al., 2015; Dvoroznáková et al., 2004; Rodrigues et al., 1995; Wen et al., 1996). Another study (Naseri et al., 2016) reported that PLGA-PEG nanoparticles loaded with albendazole sulfoxide were not more efficacious against protoscoleces of *Echinococcus granulosus*. However, while *E. granulosus* is closely related to *E. multilocularis,* protoscoleces and metacestodes are two intrinsically different parasite stages. Li et al. (2020) successfully treated mice infected with *E. multilocularis* metacestodes with magnetic PLGA-Fe nanoparticles loaded with E2-a, an alkaloid compound extracted from the traditional Tibetan medicinal plant *Sophora moorcroftiana* (Li et al., 2020).

More recently, a study published by Li et al. reported the activity of a PLGA-PEG nanoparticular formulation of the new anti-echinococcal agent H1402 (Li et al., 2023), which exhibited higher efficacy than free H1402 for hepatic AE treatment in mice following oral administration. The PLGA-PEG nanoparticles enabled targeted delivery of the anti-echinococcal agent (H1402) to the infected liver, thereby enhancing therapeutic efficacy while reducing systemic toxicity. The uniform size and spherical shape of nanoparticles facilitate their rapid penetration and extensive accumulation within the *E. multilocularis* metacestodes. Altogether, this study brought complementary data that supports us in the use of nanoparticles for AE treatment. However, some of the results are surprising, as PLGA-PEG nanoparticles are known to be poorly absorbed through the oral route (Morelli et al., 2019; Xu et al., 2015). As the same dosage of free H1402 and H1402-loaded nanoparticles was used (100 mg/kg) the biodisponibility was expected to be lower for the nanobody formulation compared to free H1402. This poor oral absorption explains that PLGA-PEG formulations currently in development for oral administration are designed with pH-sensitive architecture and ligand coating in order to improve digestive absorption (Li et al., 2022; Shi et al., 2018; T. T. Yang et al., 2022).

In summary, our study showed that PLGA-PEG-COOH nanoparticles are efficient drug delivery systems that are rapidly taken up by *E. multilocularis* metacestodes *in vitro*. PLGA-PEG-COOH nanoparticles acquired mefloquine with a loading rate of 69% allowing optimal production. Formulations are stable over time, which renders them useful for therapeutic purposes and promising candidates for drug delivery during AE treatment. Due to the intrinsic side effects of the drug and the

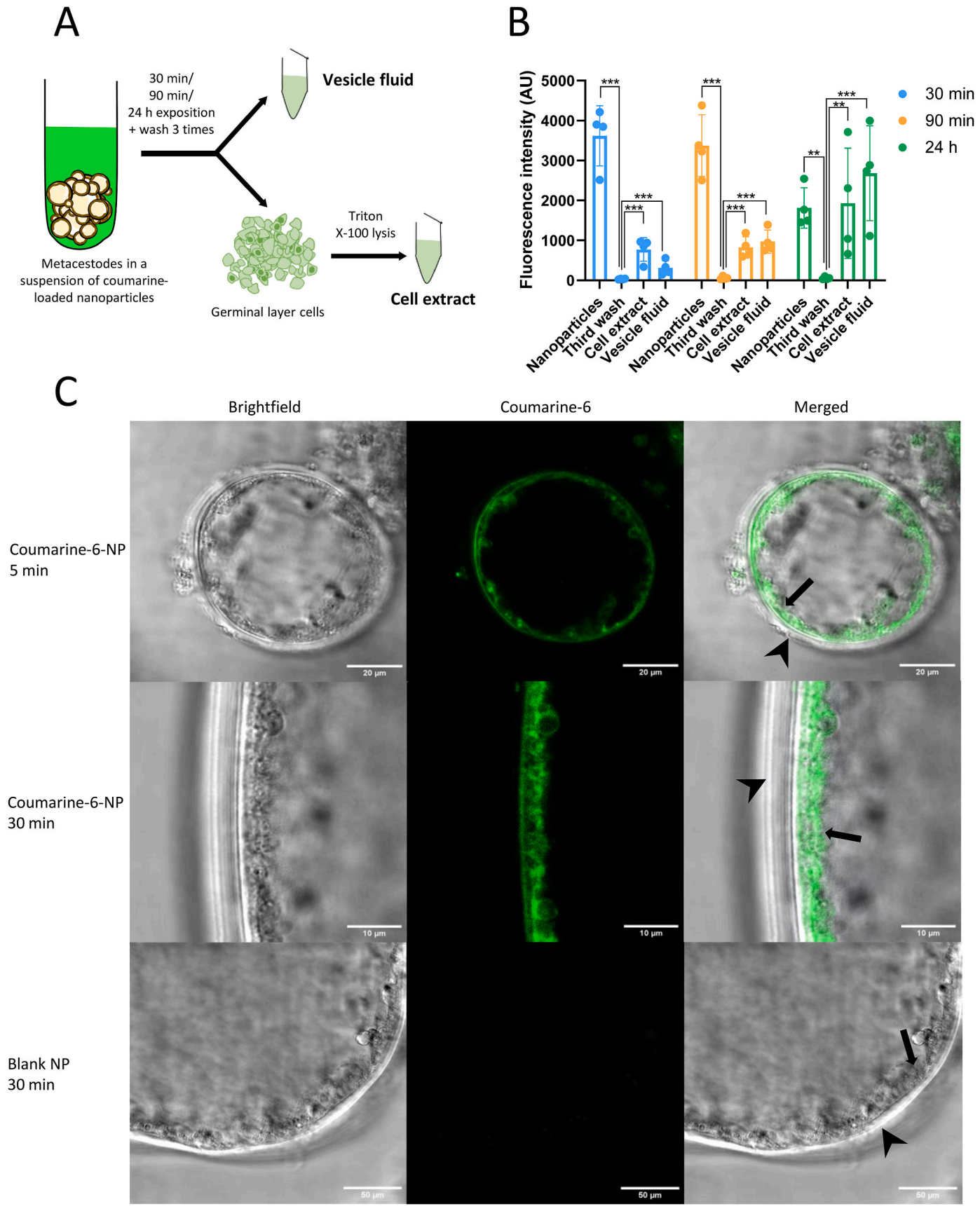

(caption on next page)

Fig. 3. Fluorimetry of supernatants and metacestode fractions after exposition to coumarine-6-loaded PLGA-PEG-COOH nanoparticles. (A) *E. multilocularis* metacestodes were exposed to coumarine-6-loaded nanoparticles during 30 min, 90 min or 24 h, washed, and vesicle fluid and germinal layer cells were obtained by mechanical disruption of the vesicles. Four samples were collected: the solution of nanoparticles, the third wash solution, the extract of germinal layer cells and the vesicle fluid. (B) Plot showing fluorescence intensity at 520 nm under 450 nm excitation of the previously collected samples. For each condition, plot shows pooled data from 4 independent experiments, mean and SD. Data were compared using two-way ANOVA and *post-hoc* Tukey's multiple comparison test. $^{**}p < 0.01$, $^{***}p < 0.001$. (C) Confocal microscopy of *Echinococcus multilocularis* vesicles. Metacestodes were exposed to either coumarine-6-loaded PLGA-PEG-COOH nanoparticles (coumarine-6-NP) during 5 min or 30 min, or blank PLGA-PEG-COOH nanoparticles (blank NP) during 30 min. When exposed to coumarine-6-NP, fluorescence can be observed in the inner germinal layer (arrows), and not the outer laminated layer (arrowheads). Observations were representative of 2 independent experiments.

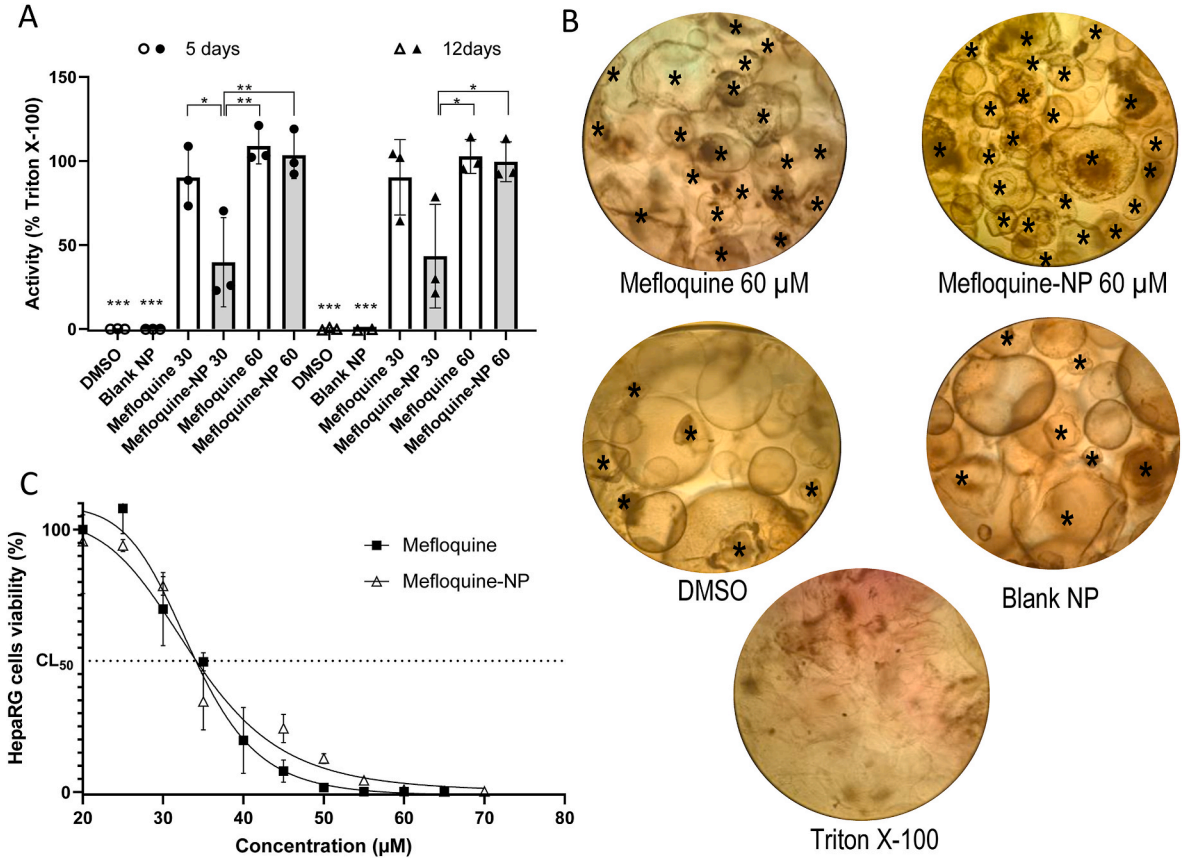

Fig. 4. Antiparasitic activity and toxicity of mefloquine loaded in PLGA-PEG-COOH nanoparticles. (A) Plot showing *in vitro* release of EmPGI expressed in percentage of the positive control (Triton X-100) after 5 days and 12 days of treatment. Representative data from two independent experiments with three biological replica each. Data were compared using one-way ANOVA and *post-hoc* Bonferroni's multiple comparison test. $^{*}p < 0.05$, $^{**}p < 0.001$, $^{***}p < 0.001$. For DMSO and unloaded PLGA-PEG-COOH nanoparticles (blank NP), statistical significance indicates comparison within the same timepoint with 30 µM and 60 µM free mefloquine and 60 µM mefloquine-loaded PLGA-PEG-COOH nanoparticles (mefloquine-NP) conditions. (B) Pictures of the vesicles after 12 days of *in vitro* exposition to the indicated treatment, by optical microscopy at 100 fold magnification. Vesicles were broken when exposed to 60 µM mefloquine, 60 µM mefloquine-NP and Triton X-100. Morphology of vesicles was not altered when exposed to DMSO or blank NP. Pictures are representative of two experiments. Altered vesicles were annotated with an asterisk. (C) Dose-response curve for viability of HepaRG cells exposed 48h to free and mefloquine-loaded PLGA-PEG-COOH nanoparticles. Obtained from one experiment. Each plot shows mean and SD.

observed cytotoxicity, however, mefloquine-loaded PLGA-PEG-COOH nanoparticles require a targeting strategy, which is currently being developed. These results have paved the way for the development of similar formulations using either mefloquine derivatives or other compounds that exhibit lower toxicity on human cells (Rufener et al., 2018b). Future pharmacokinetic and –dynamic studies in animal models will show if these promises will hold up also in an *in vivo* setting.

CRediT authorship contribution statement

Brice Autier: Writing – original draft, Visualization, Investigation, Formal analysis, Data curation. **Alexis Verger:** Writing – review & editing, Methodology, Investigation, Formal analysis, Data curation. **Charleen Plaisse:** Investigation, Formal analysis. **Christelle Manuel:** Investigation, Data curation. **Marylène Chollet-Krugler:** Methodology, Investigation, Formal analysis. **Matias Preza:** Investigation, Formal analysis. **Britta Lundstroem-Stadelmann:** Writing – review & editing, Validation, Supervision, Resources, Methodology, Conceptualization. **Marian Amela-Cortes:** Writing – review & editing, Methodology. **Caroline Aninat:** Writing – review & editing, Resources. **Michel Samson:** Project administration, Funding acquisition. **Nolwenn Brandhonneur:** Writing – review & editing, Visualization, Validation, Conceptualization. **Sarah Dion:** Writing – review & editing, Validation, Supervision, Resources, Project administration, Methodology, Investigation, Funding acquisition, Conceptualization.

Declaration of competing interest

The authors declare the following financial interests/personal relationships which may be considered as potential competing interests:

Britta Lundstroem-Stadelmann reports financial support was provided by Swiss National Science Foundation. If there are other authors, they declare that they have no known competing financial interests or personal relationships that could have appeared to influence the work reported in this paper.

Data availability

Data will be made available on request.

Acknowledgments

Authors have no conflict of interest to declare.

This study was funded by Université Rennes 1 (“Défis scientifiques”, “Projet inter-UMR” and “Financement BIOSIT” grants) and Inserm “Projet de Recherche International” (PRI) grant (NANOTHERA-ECHINO). Contribution of Britta Lundstroem-Stadelmann was supported by the SNSF project 310030_192072.

The authors thank the whole Irset Team 2. We thank the SFR Biosit UMS CNRS 3480-INSERM 018, Rennes (https://biosit.univ-rennes1.fr/) MRIc platform and the Arche animal house platform. We also thank Andrew Hemphill for his careful proofreading of langage.

References

Abulaihaiti, M., Wu, X.-W., Qiao, L., Lv, H.-L., Zhang, H.-W., Aduwayi, N., Wang, Y.-J., Wang, X.-C., Peng, X.-Y., 2015. Efficacy of albendazole-chitosan microsphere-based treatment for alveolar echinococcosis in mice. PLoS Neglected Trop. Dis. 9, e0003950 https://doi.org/10.1371/journal.pntd.0003950.

Amela-Cortes, M., Roullier, V., Wolpert, C., Neubauer, S., Kessler, H., Bedel, O., Mignani, S., Marchi-Artzner, V., 2011. Stable functionalized PEGylated quantum dots micelles with a controlled stoichiometry. Chem. Commun. 47, 1246–1248. https://doi.org/10.1039/C0CC03753B.

Autier, B., Gottstein, B., Millon, L., Ramharter, M., Gruener, B., Bresson-Hadni, S., Dion, S., Robert-Gangneux, F., 2023. Alveolar echinococcosis in immunocompromised hosts. Clin. Microbiol. Infect. 29, 593–599. https://doi.org/10.1016/j.cmi.2022.12.010.

Brunetti, E., Kern, P., Vuitton, D.A., 2010. Expert consensus for the diagnosis and treatment of cystic and alveolar echinococcosis in humans. Acta Trop. 114, 1–16. https://doi.org/10.1016/j.actatropica.2009.11.001.

Burkert, S., Peters, L., Bloehdorn, J., Grüner, B., 2022. Salvage therapy for alveolar echinococcosis-a case series. Pathogens 11, 333. https://doi.org/10.3390/pathogens11030333.

Caputo, F., Clogston, J., Calzolai, L., Rösslein, M., Prina-Mello, A., 2019. Measuring particle size distribution of nanoparticle enabled medicinal products, the joint view of EUNCL and NCI-NCL. A step by step approach combining orthogonal measurements with increasing complexity. J. Contr. Release 299, 31–43. https://doi.org/10.1016/j.jconrel.2019.02.030.

Casulli, A., 2020. Recognising the substantial burden of neglected pandemics cystic and alveolar echinococcosis. Lancet Global Health 8, e470–e471. https://doi.org/10.1016/S2214-109X(20)30066-8.

Chauchet, A., Grenouillet, F., Knapp, J., Richou, C., Delabrousse, E., Dentan, C., Millon, L., Di Martino, V., Contreras, R., Deconinck, E., Blagosklonov, O., Vuitton, D. A., Bresson-Hadni, S., FrancEchino, Network, 2014. Increased incidence and characteristics of alveolar echinococcosis in patients with immunosuppression-associated conditions. Clin. Infect. Dis. 59, 1095–1104. https://doi.org/10.1093/cid/ciu520.

Dvoroznáková, E., Hrcková, G., Borosková, Z., Velebný, S., Dubinský, P., 2004. Effect of treatment with free and liposomized albendazole on selected immunological parameters and cyst growth in mice infected with *Echinococcus multilocularis*. Parasitol. Int. 53, 315–325. https://doi.org/10.1016/j.parint.2004.05.001.

Friedman, A.D., Claypool, S.E., Liu, R., 2013. The smart targeting of nanoparticles. Curr. Pharmaceut. Des. 19, 6315–6329.

Ganachaud, F., Katz, J.L., 2005. Nanoparticles and nanocapsules created using the Ouzo effect: spontaneous emulisification as an alternative to ultrasonic and high-shear devices. Chem. Phys. Chem. 6, 209–216. https://doi.org/10.1002/cphc.200400527.

Gao, H.-J., Sun, X.-D., Luo, Y.-P., Pang, H.-S., Ma, X.-M., Zhang, T., Jing, T., Hu, W., Shen, Y.-J., Cao, J.-P., 2021. Anti-echinococcal effect of verapamil involving the regulation of the calcium/calmodulin-dependent protein kinase II response in vitro and in a murine infection model. Parasites Vectors 14, 108. https://doi.org/10.1186/s13071-021-04618-4.

Ghosh, D.K., Kumar, A., Ranjan, A., 2021. Cellular targets of mefloquine. Toxicology 464, 152995. https://doi.org/10.1016/j.tox.2021.152995.

Gottstein, B., Wang, J., Boubaker, G., Marinova, I., Spiliotis, M., Müller, N., Hemphill, A., 2015. Susceptibility versus resistance in alveolar echinococcosis (larval infection with *Echinococcus multilocularis*). Vet. Parasitol. 103–109. https://doi.org/10.1016/j.vetpar.2015.07.029.

Gripon, P., Rumin, S., Urban, S., Le Seyec, J., Glaise, D., Cannie, I., Guyomard, C., Lucas, J., Trepo, C., Guguen-Guillouzo, C., 2002. Infection of a human hepatoma cell line by hepatitis B virus. Proc. Natl. Acad. Sci. USA 99, 15655–15660. https://doi.org/10.1073/pnas.232137699.

Hemer, S., Brehm, K., 2012. In vitro efficacy of the anticancer drug imatinib on *Echinococcus multilocularis* larvae. Int. J. Antimicrob. Agents 40, 458–462. https://doi.org/10.1016/j.ijantimicag.2012.07.007.

Joekel, D.E., Lundström-Stadelmann, B., Müllhaupt, B., Hemphill, A., Deplazes, P., 2018. Evaluation of kinase-inhibitors nilotinib and everolimus against alveolar echinococcosis in vitro and in a mouse model. Exp. Parasitol. 188, 65–72. https://doi.org/10.1016/j.exppara.2018.04.002.

Koziol, U., Brehm, K., 2015. Recent advances in *Echinococcus* genomics and stem cell research. Vet. Parasitol. 213, 92–102. https://doi.org/10.1016/j.vetpar.2015.07.031.

Küster, T., Kriegel, N., Boykin, D.W., Stephens, C.E., Hemphill, A., 2013. In vitro and in vivo activities of dicationic diguanidino compounds against *Echinococcus multilocularis* metacestodes. Antimicrob. Agents Chemother. 57, 3829–3835. https://doi.org/10.1128/AAC.02569-12.

Küster, T., Stadelmann, B., Hermann, C., Scholl, S., Keiser, J., Hemphill, A., 2011. In vitro and in vivo efficacies of mefloquine-based treatment against alveolar echinococcosis. Antimicrob. Agents Chemother. 55, 713–721. https://doi.org/10.1128/AAC.01392-10.

Küster, T., Stadelmann, B., Rufener, R., Risch, C., Müller, J., Hemphill, A., 2015. Oral treatments of *Echinococcus multilocularis*-infected mice with the antimalarial drug mefloquine that potentially interacts with parasite ferritin and cystatin. Int. J. Antimicrob. Agents 46, 546–551. https://doi.org/10.1016/j.ijantimicag.2015.07.016.

Lee, C.K., Atibalentja, D.F., Yao, L.E., Park, J., Kuruvilla, S., Felsher, D.W., 2022. Anti-PD-L1 F(ab) Conjugated PEG-PLGA nanoparticle enhances immune checkpoint therapy. Nanotheranostics 6, 243–255. https://doi.org/10.7150/ntno.65544.

Li, J., Qiang, H., Yang, W., Xu, Y., Feng, T., Cai, H., Wang, S., Liu, Z., Zhang, Z., Zhang, J., 2022. Oral insulin delivery by epithelium microenvironment-adaptive nanoparticles. J. Contr. Release 341, 31–43. https://doi.org/10.1016/j.jconrel.2021.11.020.

Li, Jun, Yang, Y., Han, X., Li, Jing, Tian, M., Qi, W., An, H., Wu, C., Zhang, Y., Han, S., Duan, L., Wang, W., Zhang, W., 2023. Oral delivery of anti-parasitic agent-loaded PLGA nanoparticles: enhanced liver targeting and improved therapeutic effect on hepatic alveolar echinococcosis. Int. J. Nanomed. 18, 3069–3085. https://doi.org/10.2147/IJN.S397526.

Li, Z., Zhang, G., Luo, Y., Gao, Q., Wang, J., Chen, C., Xu, X., Zhao, Y., Li, T., Ma, X., 2020. *In vivo* effect of magnetic microspheres loaded with E2-a in the treatment of alveolar echinococcosis. Sci. Rep. 10, 12589 https://doi.org/10.1038/s41598-020-69484-z.

Liance, M., Nemati, F., Bories, C., Couvreur, P., 1993. Experience with doxorubicin-bound polyisohexylcyanoacrylate nanoparticles on murine alveolar echinococcosis of the liver. Int. J. Parasitol. 23, 427–429. https://doi.org/10.1016/0020-7519(93)90023-r.

Liu, C., Fan, H., Ma, J., Ma, L., Ge, R.-L., 2021. *In vitro* and *in vivo* efficacy of thiacloprid against *Echinococcus multilocularis*. Parasites Vectors 14, 450. https://doi.org/10.1186/s13071-021-04952-7.

Loos, J.A., Dávila, V.A., Brehm, K., Cumino, A.C., 2020. Metformin suppresses development of the *Echinococcus multilocularis* larval stage by targeting the TOR pathway. Antimicrob. Agents Chemother. 64, e01808 https://doi.org/10.1128/AAC.01808-19, 19.

Lundström-Stadelmann, B., Rufener, R., Hemphill, A., 2020. Drug repurposing applied: activity of the anti-malarial mefloquine against *Echinococcus multilocularis*. Int J Parasitol Drugs Drug Resist 13, 121–129. https://doi.org/10.1016/j.ijpddr.2020.06.002.

Lundström-Stadelmann, B., Rufener, R., Ritler, D., Zurbriggen, R., Hemphill, A., 2019. The importance of being parasiticidal an update on drug development for the treatment of alveolar echinococcosis. Food Waterborne Parasitol 15, e00040. https://doi.org/10.1016/j.fawpar.2019.e00040.

Martins, A.C., Paoliello, M.M.B., Docea, A.O., Santamaria, A., Tinkov, A.A., Skalny, A.V., Aschner, M., 2021. Review of the mechanism underlying mefloquine-induced neurotoxicity. Crit. Rev. Toxicol. 51, 209–216. https://doi.org/10.1080/10408444.2021.1901258.

Memedovski, R., Preza, M., Müller, J., Kämpfer, T., Rufener, R., de Souza, M.V.N., da Silva, E.T., de Andrade, G.F., Braga, S., Uldry, A.-C., Buchs, N., Heller, M., Lundström-Stadelmann, B., 2023. Investigation of the mechanism of action of mefloquine and derivatives against the parasite *Echinococcus multilocularis*. Int J Parasitol Drugs Drug Resist 21, 114–124. https://doi.org/10.1016/j.ijpddr.2023.03.002.

Morelli, L., Gimondi, S., Sevieri, M., Salvioni, L., Guizzetti, M., Colzani, B., Palugan, L., Foppoli, A., Talamini, L., Morosi, L., Zucchetti, M., Violatto, M.B., Russo, L., Salmona, M., Prosperi, D., Colombo, M., Bigini, P., 2019. Monitoring the fate of orally administered PLGA nanoformulation for local delivery of therapeutic drugs. Pharmaceutics 11, 658. https://doi.org/10.3390/pharmaceutics11120658.

Naseri, M., Akbarzadeh, A., Spotin, A., Akbari, N.A.R., Mahami-Oskouei, M., Ahmadpour, E., 2016. Scolicidal and apoptotic activities of albendazole sulfoxide and albendazole sulfoxide-loaded PLGA-PEG as a novel nanopolymeric particle against *Echinococcus granulosus* protoscoleces. Parasitol. Res. 115, 4595–4603. https://doi.org/10.1007/s00436-016-5250-8.

Rodrigues, J.M., Bories, C., Emery, I., Fessi, H., Devissaguet, J.P., Liance, M., 1995. Development of an injectable formulation of albendazole and *in vivo* evaluation of its efficacy against *Echinococcus multilocularis* metacestode. Int. J. Parasitol. 25, 1437–1441. https://doi.org/10.1016/0020-7519(95)00055-0.

Rufener, R., Dick, L., D'Ascoli, L., Ritler, D., Hizem, A., Wells, T.N.C., Hemphill, A., Lundström-Stadelmann, B., 2018a. Repurposing of an old drug: *In vitro* and *in vivo* efficacies of buparvaquone against *Echinococcus multilocularis*. Int J Parasitol Drugs Drug Resist 8, 440–450. https://doi.org/10.1016/j.ijpddr.2018.10.011.

Rufener, R., Ritler, D., Zielinski, J., Dick, L., da Silva, E.T., da Silva Araujo, A., Joekel, D. E., Czock, D., Goepfert, C., Moraes, A.M., de Souza, M.V.N., Müller, J., Mevissen, M., Hemphill, A., Lundström-Stadelmann, B., 2018b. Activity of mefloquine and mefloquine derivatives against *Echinococcus multilocularis*. Int J Parasitol Drugs Drug Resist 8, 331–340. https://doi.org/10.1016/j.ijpddr.2018.06.004.

Schantz, P.M., Van den Bossche, H., Eckert, J., 1982. Chemotherapy for larval echinococcosis in animals and humans: report of a workshop. Z. Parasitenkd. 67, 5–26. https://doi.org/10.1007/BF00929509.

Semete, B., Booysen, L., Lemmer, Y., Kalombo, L., Katata, L., Verschoor, J., Swai, H.S., 2010. *In vivo* evaluation of the biodistribution and safety of PLGA nanoparticles as drug delivery systems. Nanomedicine 6, 662–671. https://doi.org/10.1016/j.nano.2010.02.002.

Shi, Y., Sun, X., Zhang, L., Sun, K., Li, K., Li, Y., Zhang, Q., 2018. Fc-modified exenatide-loaded nanoparticles for oral delivery to improve hypoglycemic effects in mice. Sci. Rep. 8, 726. https://doi.org/10.1038/s41598-018-19170-y.

Spicher, M., Roethlisberger, C., Lany, C., Stadelmann, B., Keiser, J., Ortega-Mora, L.M., Gottstein, B., Hemphill, A., 2008. *In vitro* and *in vivo* treatments of *Echinococcus* protoscoleces and metacestodes with artemisinin and artemisinin derivatives. Antimicrob. Agents Chemother. 52, 3447–3450. https://doi.org/10.1128/AAC.00553-08.

Stadelmann, B., Aeschbacher, D., Huber, C., Spiliotis, M., Müller, J., Hemphill, A., 2014. Profound activity of the anti-cancer drug bortezomib against *Echinococcus multilocularis* metacestodes identifies the proteasome as a novel drug target for cestodes. PLoS Neglected Trop. Dis. 8, e3352 https://doi.org/10.1371/journal.pntd.0003352.

Stadelmann, B., Küster, T., Scholl, S., Barna, F., Kropf, C., Keiser, J., Boykin, D.W., Stephens, C.E., Hemphill, A., 2011. *In vitro* efficacy of dicationic compounds and mefloquine enantiomers against *Echinococcus multilocularis* metacestodes. Antimicrob. Agents Chemother. 55, 4866–4872. https://doi.org/10.1128/AAC.00478-11.

Stadelmann, B., Rufener, R., Aeschbacher, D., Spiliotis, M., Gottstein, B., Hemphill, A., 2016. Screening of the open source malaria box reveals an early lead compound for the treatment of alveolar echinococcosis. PLoS Neglected Trop. Dis. 10, e0004535 https://doi.org/10.1371/journal.pntd.0004535.

Stadelmann, B., Scholl, S., Müller, J., Hemphill, A., 2010a. Application of an in vitro drug screening assay based on the release of phosphoglucose isomerase to determine the structure-activity relationship of thiazolides against *Echinococcus multilocularis* metacestodes. J. Antimicrob. Chemother. 65, 512–519. https://doi.org/10.1093/jac/dkp490.

Stadelmann, B., Spiliotis, M., Müller, J., Scholl, S., Müller, N., Gottstein, B., Hemphill, A., 2010b. *Echinococcus multilocularis* phosphoglucose isomerase (EmPGI): a glycolytic enzyme involved in metacestode growth and parasite-host cell interactions. Int. J. Parasitol. 40, 1563–1574. https://doi.org/10.1016/j.ijpara.2010.05.009.

Stettler, M., Siles-Lucas, M., Sarciron, E., Lawton, P., Gottstein, B., Hemphill, A., 2001. *Echinococcus multilocularis* alkaline phosphatase as a marker for metacestode damage induced by in vitro drug treatment with albendazole sulfoxide and albendazole sulfone. Antimicrob. Agents Chemother. 45, 2256–2262. https://doi.org/10.1128/AAC.45.8.2256-2262.2001.

Venier-Julienne, M.C., Benoît, J.P., 1996. Preparation, purification and morphology of polymeric nanoparticles as drug carriers. Pharm. Acta Helv. 71, 121–128. https://doi.org/10.1016/0031-6865(95)00059-3.

Verger, A., Dollo, G., Martinais, S., Molard, Y., Cordier, S., Amela-Cortes, M., Brandhonneur, N., 2022. Molybdenum-iodine cluster loaded polymeric nanoparticles allowing a coupled therapeutic action with low side toxicity for treatment of ovarian cancer. J. Pharmaceut. Sci. S0022–3549 (22) https://doi.org/10.1016/j.xphs.2022.09.010, 00413–0.

Vuitton, D.A., McManus, D.P., Rogan, M.T., Romig, T., Gottstein, B., Naidich, A., Tuxun, T., Wen, H., Silva, A.M. da, Vuitton, D.A., McManus, D.P., Romig, T., Rogan, M.R., Gottstein, B., Silva, A.M. da, Wen, H., Naidich, A., Tuxun, T., Avcioglu, A., Boufana, B., Budke, C., Casulli, A., Güven, E., Hillenbrand, A., Jalousian, F., Jemli, M.H., Knapp, J., Laatamna, A., Lahmar, S., Naidich, A., Rogan, M.T., Sadjjadi, S.M., Schmidberger, J., Amri, M., Bellanger, A.-P., Benazzouz, S., Brehm, K., Hillenbrand, A., Jalousian, F., Kachani, M., Labsi, M., Masala, G., Silva, A.M. da, Seyed, M.S., Soufli, I., Touil-Boukoffa, C., Wang, J., Zeyhle, E., Aji, T., Akhan, O., Bresson-Hadni, S., Dziri, C., Gräter, T., Grüner, B., Haïf, A., Hillenbrand, A., Koch, S., Rogan, M.T., Tamarozzi, F., Tuxun, T., Giraudoux, P., Torgerson, P., Vizcaychipi, K., Xiao, N., Altintas, N., Lin, R., Millon, L., Zhang, W., Achour, K., Fan, H., Junghanss, T., Mantion, G.A., 2020. International consensus on terminology to be used in the field of echinococcoses. Parasite 27, 41. https://doi.org/10.1051/parasite/2020024.

Vuitton, D.A., Zhang, S.L., Yang, Y., Godot, V., Beurton, I., Mantion, G., Bresson-Hadni, S., 2006. Survival strategy of *Echinococcus multilocularis* in the human host. Parasitol. Int. 55, S51–S55. https://doi.org/10.1016/j.parint.2005.11.007.

Wang, Y., Qin, B., Xia, G., Choi, S.H., 2021. FDA's poly (lactic-Co-glycolic acid) research program and regulatory outcomes. AAPS J. 23, 92. https://doi.org/10.1208/s12248-021-00611-y.

Wen, H., New, R.R., Muhmut, M., Wang, J.H., Wang, Y.H., Zhang, J.H., Shao, Y.M., Craig, P.S., 1996. Pharmacology and efficacy of liposome-entrapped albendazole in experimental secondary alveolar echinococcosis and effect of co-administration with cimetidine. Parasitology 113 (Pt 2), 111–121. https://doi.org/10.1017/s003118200006635x.

Xu, Q., Ensign, L.M., Boylan, N.J., Schön, A., Gong, X., Yang, J.-C., Lamb, N.W., Cai, S., Yu, T., Freire, E., Hanes, J., 2015. Impact of surface polyethylene glycol (PEG) density on biodegradable nanoparticle transport in mucus *ex vivo* and distribution *in vivo*. ACS Nano 9, 9217–9227. https://doi.org/10.1021/acsnano.5b03876.

Yang, N., Ma, W., Ke, Y., Liu, H., Chu, J., Sun, L., Lü, G., Bi, X., Lin, R., 2022. Transplantation of adipose-derived stem cells ameliorates *Echinococcus multilocularis*-induced liver fibrosis in mice. PLoS Neglected Trop. Dis. 16, e0010175 https://doi.org/10.1371/journal.pntd.0010175.

Yang, T., Wang, A., Nie, D., Fan, W., Jiang, X., Yu, M., Guo, S., Zhu, C., Wei, G., Gan, Y., 2022. Ligand-switchable nanoparticles resembling viral surface for sequential drug delivery and improved oral insulin therapy. Nat. Commun. 13, 6649. https://doi.org/10.1038/s41467-022-34357-8.

Zhang, D., Liu, L., Wang, J., Zhang, H., Zhang, Z., Xing, G., Wang, X., Liu, M., 2022. Drug-loaded PEG-PLGA nanoparticles for cancer treatment. Front. Pharmacol. 13, 990505 https://doi.org/10.3389/fphar.2022.990505.